

Chirality density wave of the 'hidden order' phase in URu₂Si₂

Sciencexpress DOI: 10.1126/science.1259729

H.-H. Kung, R. E. Baumbach, E. D. Bauer, V. K. Thorsmølle, W.-L. Zhang,
K. Haule, J. A. Mydosh & G. Blumberg

A second-order phase transition is associated with emergence of an "order parameter" and a spontaneous symmetry breaking. For the heavy fermion superconductor URu₂Si₂, the symmetry of the order parameter associated with its ordered phase below 17.5 K has remained ambiguous despite 30 years of research, and hence is called "hidden order" (HO). Here we use polarization resolved Raman spectroscopy to specify the symmetry of the low energy excitations above and below the HO transition. These excitations involve transitions between interacting heavy uranium 5*f* orbitals, responsible for the broken symmetry in the HO phase. From the symmetry analysis of the collective mode, we determine that the HO parameter breaks local vertical and diagonal reflection symmetries at the uranium sites, resulting in crystal field states with distinct chiral properties, which order to a commensurate chirality density wave ground state.

March 3, 2015

Layout

- 1 URu₂Si₂
 - f*-electrons
 - Hidden order (HO) in URu₂Si₂
- 2 Crystal field states
 - Atomic configuration
 - Crystal symmetry
- 3 Polarization resolved Raman spectroscopy
 - Results
 - Hidden order

- Uranium is intriguing, even *natural or depleted* (99.5% ²³⁸U)

- Uranium is intriguing, even *natural or depleted* (99.5% ²³⁸U)
- Unlike ²³⁵U, it is not *fissile*, mild α radioactivity

- Uranium is intriguing, even *natural or depleted* (99.5% ²³⁸U)
- Unlike ²³⁵U, it is not *fissile*, mild α radioactivity
- Compounds are fabricated and studied in university labs with *minimal* safety precautions

- Uranium is intriguing, even *natural or depleted* (99.5% ²³⁸U)
- Unlike ²³⁵U, it is not *fissile*, mild α radioactivity
- Compounds are fabricated and studied in university labs with *minimal* safety precautions
- Unusual behaviors of U compounds are due to the 5f electrons

- Uranium is intriguing, even *natural or depleted* (99.5% ²³⁸U)
- Unlike ²³⁵U, it is not *fissile*, mild α radioactivity
- Compounds are fabricated and studied in university labs with *minimal* safety precautions
- Unusual behaviors of U compounds are due to the 5*f* electrons
- For U *f* electrons: the exchange interaction, the spin orbit interaction, intra-atomic *f-f* Coulomb interaction, and the 5*f* bandwidth are all on the SAME energy scale

- Uranium is intriguing, even *natural or depleted* (99.5% ²³⁸U)
- Unlike ²³⁵U, it is not *fissile*, mild α radioactivity
- Compounds are fabricated and studied in university labs with *minimal* safety precautions
- Unusual behaviors of U compounds are due to the 5*f* electrons
- For U *f* electrons: the exchange interaction, the spin orbit interaction, intra-atomic *f-f* Coulomb interaction, and the 5*f* bandwidth are all on the SAME energy scale
- U lies directly on the border between localized and itinerant 5*f* wavefunctions (*heavy fermion*)

- Uranium is intriguing, even *natural or depleted* (99.5% ²³⁸U)
- Unlike ²³⁵U, it is not *fissile*, mild α radioactivity
- Compounds are fabricated and studied in university labs with *minimal* safety precautions
- Unusual behaviors of U compounds are due to the 5f electrons
- For U f electrons: the exchange interaction, the spin orbit interaction, intra-atomic f-f Coulomb interaction, and the 5f bandwidth are all on the SAME energy scale
- U lies directly on the border between localized and itinerant 5f wavefunctions (*heavy fermion*)
- Ionic U can adopt six different valences, usually U⁴⁺ with two 5f electrons

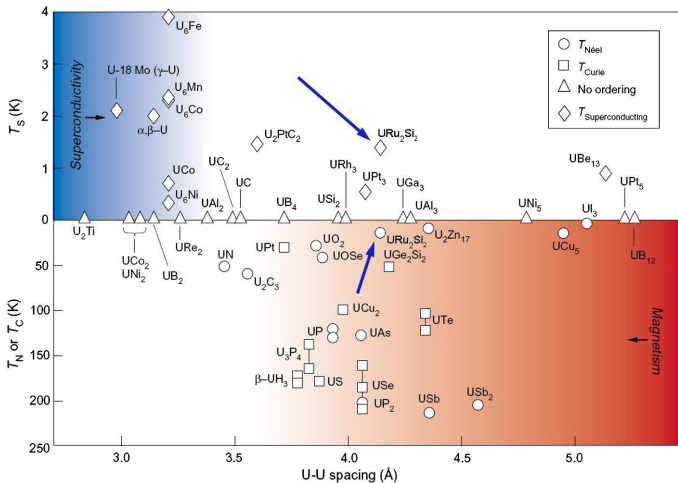


Figure : The Hill plot for various U based intermetallic compounds. Bottom arrow indicates hidden-order (HO) transition temperature T_0 and the top arrow indicates its superconducting transition temperature (Hill, 1970).

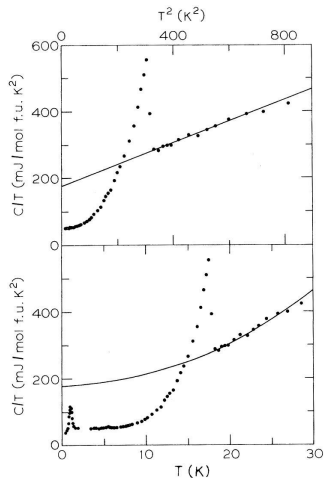


Figure : Electronic specific heat as a function of temperature for URu₂Si₂ (Palstra et al., PRL 1985)

- Jump discontinuity in specific heat signals *second-order* phase transition

- Jump discontinuity in specific heat signals *second-order* phase transition
- Exponential specific heat ($e^{-\Delta/(k_B T)}$) below T_0 implies gap Δ opening up in the electronic spectrum in th HO phase

- Jump discontinuity in specific heat signals *second-order* phase transition
- Exponential specific heat ($e^{-\Delta/(k_B T)}$) below T_0 implies gap Δ opening up in the electronic spectrum in th HO phase
- Fermi surface is destroyed

- Jump discontinuity in specific heat signals *second-order* phase transition
- Exponential specific heat ($e^{-\Delta/(k_B T)}$) below T_0 implies gap Δ opening up in the electronic spectrum in th HO phase
- Fermi surface is destroyed
- Thermal expansion experiments suggest a net volume increase in the HO phase indicating significant coupling of the HO phase with the lattice

- Jump discontinuity in specific heat signals *second-order* phase transition
- Exponential specific heat ($e^{-\Delta/(k_B T)}$) below T_0 implies gap Δ opening up in the electronic spectrum in th HO phase
- Fermi surface is destroyed
- Thermal expansion experiments suggest a net volume increase in the HO phase indicating significant coupling of the HO phase with the lattice
- Q: What is the symmetry of the associate order parameter ? unknown for three decades (since 1984)

- Jump discontinuity in specific heat signals *second-order* phase transition
- Exponential specific heat ($e^{-\Delta/(k_B T)}$) below T_0 implies gap Δ opening up in the electronic spectrum in th HO phase
- Fermi surface is destroyed
- Thermal expansion experiments suggest a net volume increase in the HO phase indicating significant coupling of the HO phase with the lattice
- Q: What is the symmetry of the associate order parameter ?
unknown for three decades (since 1984)
- A: commensurate chirality density wave

Layout

- 1 URu₂Si₂
f-electrons
Hidden order (HO) in URu₂Si₂
- 2 Crystal field states
Atomic configuration
Crystal symmetry
- 3 Polarization resolved Raman spectroscopy
Results
Hidden order

- In the dominant atomic configuration, the orbital angular momentums and spins of the two quasi-localized U-5*f* electrons add up to total momentum $4\hbar$, having nine-fold degeneracy.

- In the dominant atomic configuration, the orbital angular momentums and spins of the two quasi-localized U-5*f* electrons add up to total momentum $4\hbar$, having nine-fold degeneracy.
- Suppose a free atom or ion with all shells filled but one

- In the dominant atomic configuration, the orbital angular momentums and spins of the two quasi-localized U-5*f* electrons add up to total momentum $4\hbar$, having nine-fold degeneracy.
- Suppose a free atom or ion with all shells filled but one
- Single electrons levels are characterized by orbital angular momentum l , $l_z \in \{-l, l\}$

- In the dominant atomic configuration, the orbital angular momentums and spins of the two quasi-localized U-5*f* electrons add up to total momentum $4\hbar$, having nine-fold degeneracy.
- Suppose a free atom or ion with all shells filled but one
- Single electrons levels are characterized by orbital angular momentum l , $l_z \in \{-l, l\}$
- If the electrons did not interact with one another the ionic ground state would be degenerate $2 \times (2l + 1)$

- In the dominant atomic configuration, the orbital angular momentums and spins of the two quasi-localized U-5*f* electrons add up to total momentum $4\hbar$, having nine-fold degeneracy.
- Suppose a free atom or ion with all shells filled but one
- Single electrons levels are characterized by orbital angular momentum l , $l_z \in \{-l, l\}$
- If the electrons did not interact with one another the ionic ground state would be degenerate $2 \times (2l + 1)$
- Presence of $e - e$ Coulomb interactions and electron spin orbit interactions considerably lift the degeneracy as revealed by atomic spectroscopies

- Can find the low energy states using Hund's rules, derived using detailed electronic state calculations using accurate wavefunctions

- Can find the low energy states using Hund's rules, derived using detailed electronic state calculations using accurate wavefunctions
- Hund's First Rule: Out of the many states that can be formed by placing n electrons into $2(2l + 1)$ states of the partially filled shell, those that lie lowest in energy have the largest total spin S , consistent with the exclusion principle

- Can find the low energy states using Hund's rules, derived using detailed electronic state calculations using accurate wavefunctions
- Hund's First Rule: Out of the many states that can be form by placing n electrons into $2(2l + 1)$ states of the partially filled shell, those that lie lowest in energy have the largest total spin S , consistent with the exclusion principle
- Largest value S can have is the largest magnitude S_z can have

- Can find the low energy states using Hund's rules, derived using detailed electronic state calculations using accurate wavefunctions
- Hund's First Rule: Out of the many states that can be formed by placing n electrons into $2(2l + 1)$ states of the partially filled shell, those that lie lowest in energy have the largest total spin S , consistent with the exclusion principle
- Largest value S can have is the largest magnitude S_z can have
- If number of electrons $n \leq 2l + 1$, all electrons can have parallel spins respecting the exclusion principle

- Can find the low energy states using Hund's rules, derived using detailed electronic state calculations using accurate wavefunctions
- Hund's First Rule: Out of the many states that can be formed by placing n electrons into $2(2l + 1)$ states of the partially filled shell, those that lie lowest in energy have the largest total spin S , consistent with the exclusion principle
- Largest value S can have is the largest magnitude S_z can have
- If number of electrons $n \leq 2l + 1$, all electrons can have parallel spins respecting the exclusion principle
- $5f^2$: implies $l = 3$, $n = 2$, therefore $S = 1$

- Hund's Second Rule: The total orbital angular momentum L of the lowest-lying states has the largest value that is consistent with Hund's first rule and the exclusion principle

- Hund's Second Rule: The total orbital angular momentum L of the lowest-lying states has the largest value that is consistent with Hund's first rule and the exclusion principle
- Largest value L can have is the largest magnitude L_z can have

- Hund's Second Rule: The total orbital angular momentum L of the lowest-lying states has the largest value that is consistent with Hund's first rule and the exclusion principle
- Largest value L can have is the largest magnitude L_z can have
- $5f^2$: the first electron goes to level with $|l_z| = l$, the second must have same spin as the first (according to the first rule), so the best it can do is to go to $|l_z| = l - 1$

- Hund's Second Rule: The total orbital angular momentum L of the lowest-lying states has the largest value that is consistent with Hund's first rule and the exclusion principle
- Largest value L can have is the largest magnitude L_z can have
- $5f^2$: the first electron goes to level with $|l_z| = l$, the second must have same spin as the first (according to the first rule), so the best it can do is to go to $|l_z| = l - 1$
- Thus we have $L = l + (l - 1) = 5$

- Hund's Second Rule: The total orbital angular momentum L of the lowest-lying states has the largest value that is consistent with Hund's first rule and the exclusion principle
- Largest value L can have is the largest magnitude L_z can have
- $5f^2$: the first electron goes to level with $|l_z| = l$, the second must have same spin as the first (according to the first rule), so the best it can do is to go to $|l_z| = l - 1$
- Thus we have $L = l + (l - 1) = 5$
- The first two rules only determine the values of L and S , what about total angular momentum $J = L + S$, which can take all integral values between $|L - S|$ and $L + S$

- Hund's Third Rule: Spin-orbit coupling $\lambda L \cdot S$ favors maximum J (parallel L and S) if λ is negative and minimum J (antiparallel L and S) if λ is positive

- Hund's Third Rule: Spin-orbit coupling $\lambda L \cdot S$ favors maximum J (parallel L and S) if λ is negative and minimum J (antiparallel L and S) if λ is positive
- λ is positive for shells that are less than half filled

- Hund's Third Rule: Spin-orbit coupling $\lambda L \cdot S$ favors maximum J (parallel L and S) if λ is negative and minimum J (antiparallel L and S) if λ is positive
- λ is positive for shells that are less than half filled
- $5f^2$: implies $J = |L - S| = 4$

- Hund's Third Rule: Spin-orbit coupling $\lambda L \cdot S$ favors maximum J (parallel L and S) if λ is negative and minimum J (antiparallel L and S) if λ is positive
- λ is positive for shells that are less than half filled
- $5f^2$: implies $J = |L - S| = 4$
- Nine fold degeneracy can be labeled using $J_z \in \{-4, 4\}$

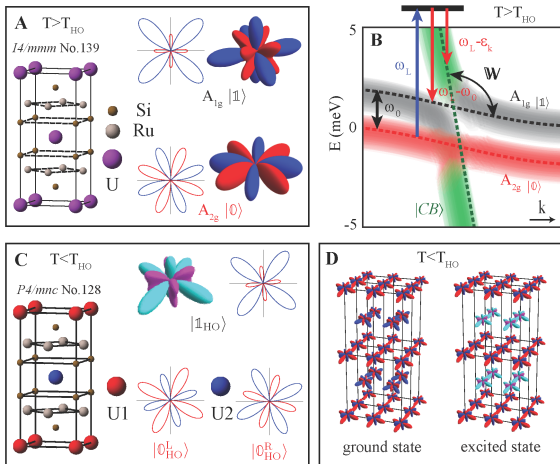


Figure : Schematics of the local symmetry and band structure of the quasi-localized states in the minimal model, above and below T_{HO} . **(A)** The crystal structure of URu₂Si₂ in the paramagnetic phase. Presented in 3D and xy-plane cut are wave functions that show the symmetry of the A_{2g} state $|\uparrow\rangle$ and A_{1g} state $|\uparrow\rangle$, where the positive (negative) amplitude is denoted by red (blue) color. The A_{1g} state is symmetric with respect to the vertical and diagonal reflections, while the A_{2g} state is antisymmetric with respect to these reflections.

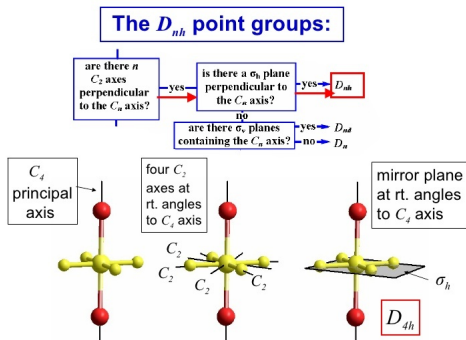


Figure : URu₂Si₂ crystallizes in a body-centered tetragonal structure belonging to the D_{4h} point group.

Table S1: The crystal field states of U-5*f* electrons with two electrons in the $j = 5/2$ subshell, categorized by irreducible representations (IRR) of the D_{4h} group. These states have total angular momentum $J = 4$ and magnetic quantum number M_J runs from $-4 \cdots 4$. The states on the right hand site are labeled by their M_J value, e.g. $|0\rangle \equiv |J = 4, M_J = 0\rangle$

IRR	state
$A_{2g} (\Gamma_2)$	$ 0\rangle = \frac{i}{\sqrt{2}}(4\rangle - -4\rangle)$
$A_{1g} (\Gamma_1^{(1)})$	$ 1\rangle = \frac{\cos \theta}{\sqrt{2}}(4\rangle + -4\rangle) - \sin \theta 0\rangle$
$A_{1g} (\Gamma_1^{(2)})$	$ 2\rangle = \frac{\sin \theta}{\sqrt{2}}(4\rangle + -4\rangle) + \cos \theta 0\rangle$
$E_g (\Gamma_{5,1}^{(1)})$	$ 3\rangle = \cos \phi -3\rangle + \sin \phi 1\rangle$
$E_g (\Gamma_{5,2}^{(1)})$	$ 4\rangle = \cos \phi 3\rangle + \sin \phi -1\rangle$
$E_g (\Gamma_{5,1}^{(2)})$	$ 5\rangle = \sin \phi -3\rangle - \cos \phi 1\rangle$
$E_g (\Gamma_{5,2}^{(2)})$	$ 6\rangle = \sin \phi 3\rangle - \cos \phi -1\rangle$
$B_{1g} (\Gamma_3)$	$ 7\rangle = \frac{1}{\sqrt{2}}(2\rangle + -2\rangle)$
$B_{2g} (\Gamma_4)$	$ 8\rangle = \frac{i}{\sqrt{2}}(2\rangle - -2\rangle)$

Figure : In the crystal environment of URu₂Si₂, the nine states split into seven energy levels denoted by irreducible representations of the D_{4h} group: 5 singlet states $2A_{1g} \oplus A_{2g} \oplus B_{1g} \oplus B_{2g}$ and 2 doublet states $2E_g$.

Mulliken Labels for Representations

- **Non-Degenerate Representations = A or B**

Character under identity $E = 1$; (symmetric)

Character under Principal axis = 1 then Symbol = **A**

Character under identity $E = 1$; (symmetric)

Character under Principal axis = -1 (anti-symmetric)

Symbol = **B**

When symmetric to inversion (i): add **g** = gerade (e.g. A_{1g})

When anti-symmetric to inversion: add **u** = ungerade (A_{1u})

- **Degenerate Representations:**

Doublet: Symbol = **E** (Example: E_g in O_h point group)

Triplet: Symbol = **T** (Example: T_{2g} in O_h point group)

Figure : Low energy minimal model including lowest three states only have A_{1g} and A_{2g} states

Layout

- 1 URu₂Si₂
 - f*-electrons
 - Hidden order (HO) in URu₂Si₂
- 2 Crystal field states
 - Atomic configuration
 - Crystal symmetry
- 3 Polarization resolved Raman spectroscopy
 - Results
 - Hidden order

- Inelastic scattering of monochromatic light

- Inelastic scattering of monochromatic light
- Laser light interacts with lattice vibrations and the scattered photons are shifted up or down in energy providing informations about vibrational modes

- Inelastic scattering of monochromatic light
- Laser light interacts with lattice vibrations and the scattered photons are shifted up or down in energy providing informations about vibrational modes
- They perform Raman in various geometries. The six proper scattering geometries are denoted as $\mathbf{e}_s \mathbf{e}_i = XX, XY, X'X', X'Y', RR$ and RL , with \mathbf{e}_i being the direction vector for incident light polarization, and \mathbf{e}_s being the scattered light polarization. $X=[100]$, $Y=[010]$ are aligned along crystallographic axes, $X'=[110]$, $Y'=[1\bar{1}0]$ are aligned 45° to the a -axes, $R=(X+iY)/\sqrt{2}$ and $L=(X-iY)/\sqrt{2}$ are right and left circularly polarized light

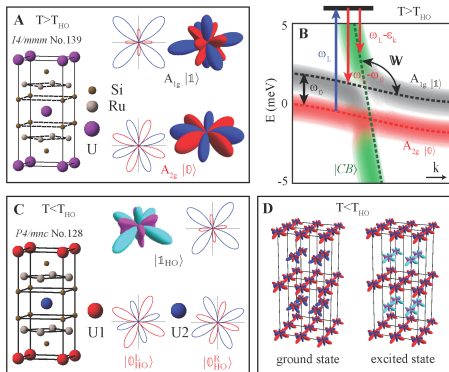


Figure : (B) Schematic of the band structure of a minimal model in the paramagnetic state. The green dashed line denotes the conduction band $|CB\rangle$, the red and black dashed lines denote crystal field states of the U $5f$ electrons: the ground state $|0\rangle$ and the first excited state $|1\rangle$. A cartoon of the Raman process is shown, where the blue and red arrows denote the incident and scattered light, respectively. ω_L is the incoming photon energy (not in scale), W is the hybridization strength between $|1\rangle$ and $|CB\rangle$, ω_0 and ϵ_k are the resonance energies for $|0\rangle \rightarrow |1\rangle$ and $|0\rangle \rightarrow |CB\rangle$, respectively.

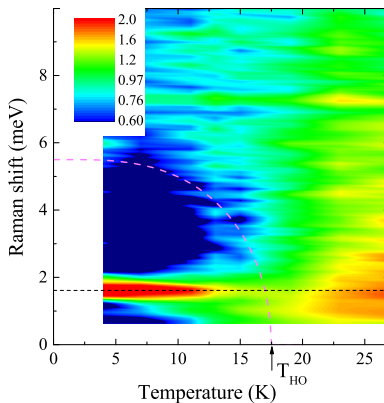


Figure : Raman response in the XY scattering geometry as function of temperature and Raman shift energy. The contour plot shows the temperature evolution of the low energy Raman response in the XY scattering geometry. A sharp excitation at 1.6 meV (indicated by the black dashed line) emerges below T_{HO} . The mode's full width at half maximum decreases on cooling to about 0.3 meV at 4 K. A gap-like suppression develops to a magnitude of about 6 meV at 4 K. The pink dashed line shows the temperature dependence of a gap expected from a mean-field BCS model with a transition temperature of 17.5 K.

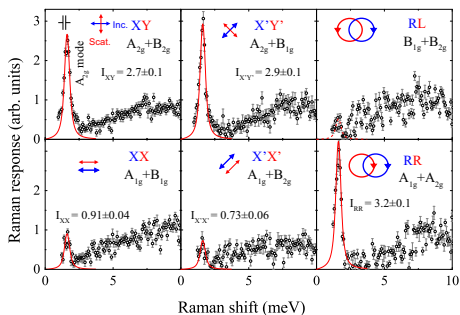


Figure : The Raman response in six proper scattering geometries at 7 K. The data are shown in black circles, where the error bars show one standard deviation. The red solid lines are fits of the in-gap mode to a Lorentzian, and the fitted intensity using the method of maximum likelihood is shown in each panel. By decomposition, the in-gap mode intensity in each symmetry channels are: $I_{A_{2g}} = 2.6 \pm 0.1$, $I_{A_{1g}} = 0.7 \pm 0.1$, $I_{B_{1g}} = 0.3 \pm 0.1$, and $I_{B_{2g}} = 0.1 \pm 0.1$. The full width at half maximum of the in-gap mode is about 0.5 meV at 7 K (deconvoluted with instrumental resolution of 0.15 meV, shown in the XY panel)

- The intense in-gap mode is observed in all scattering geometries containing A_{2g} symmetry.

- The intense in-gap mode is observed in all scattering geometries containing A_{2g} symmetry.
- The mode can be interpreted as a $\omega_0 = 1.6$ meV resonance between the $|0\rangle$ and $|1\rangle$ quasi-localized states, which can only appear in the A_{2g} channel of the D_{4h} group.

- The intense in-gap mode is observed in all scattering geometries containing A_{2g} symmetry.
- The mode can be interpreted as a $\omega_0 = 1.6$ meV resonance between the $|0\rangle$ and $|1\rangle$ quasi-localized states, which can only appear in the A_{2g} channel of the D_{4h} group.
- A weaker intensity is also observed at the same energy in XX and X'X' geometries commonly containing the excitations of the A_{1g} symmetry, and a much weaker intensity is barely seen within the experimental uncertainty in RL geometry.

- The intense in-gap mode is observed in all scattering geometries containing A_{2g} symmetry.
- The mode can be interpreted as a $\omega_0 = 1.6$ meV resonance between the $|0\rangle$ and $|1\rangle$ quasi-localized states, which can only appear in the A_{2g} channel of the D_{4h} group.
- A weaker intensity is also observed at the same energy in XX and X'X' geometries commonly containing the excitations of the A_{1g} symmetry, and a much weaker intensity is barely seen within the experimental uncertainty in RL geometry.
- The in-gap mode intensity in the A_{1g} channel is about four times weaker than in the A_{2g} channel.

- The observation of this intensity “leakage” into forbidden scattering geometries implies the lowering of symmetry in the HO phase, allowing some of the irreducible representations of D_{4h} point group to mix.

- The observation of this intensity “leakage” into forbidden scattering geometries implies the lowering of symmetry in the HO phase, allowing some of the irreducible representations of \mathbb{D}_{4h} point group to mix.
- For example, the ω_0 mode intensity “leakage” from the A_{2g} into the A_{1g} channel implies that the irreducible representation A_{1g} and A_{2g} of the \mathbb{D}_{4h} point group merge into the A_g representation of the lower group \mathbb{C}_{4h} .

- The observation of this intensity “leakage” into forbidden scattering geometries implies the lowering of symmetry in the HO phase, allowing some of the irreducible representations of \mathbb{D}_{4h} point group to mix.
- For example, the ω_0 mode intensity “leakage” from the A_{2g} into the A_{1g} channel implies that the irreducible representation A_{1g} and A_{2g} of the \mathbb{D}_{4h} point group merge into the A_g representation of the lower group \mathbb{C}_{4h} .
- This signifies the breaking of the local vertical and diagonal reflection symmetries at the uranium sites in the HO phase.

- The observation of this intensity “leakage” into forbidden scattering geometries implies the lowering of symmetry in the HO phase, allowing some of the irreducible representations of \mathbb{D}_{4h} point group to mix.
- For example, the ω_0 mode intensity “leakage” from the A_{2g} into the A_{1g} channel implies that the irreducible representation A_{1g} and A_{2g} of the \mathbb{D}_{4h} point group merge into the A_g representation of the lower group \mathbb{C}_{4h} .
- This signifies the breaking of the local vertical and diagonal reflection symmetries at the uranium sites in the HO phase.
- Similarly, the tiny intensity leakage into the RL scattering geometry measure the strength of orthorhombic distortion due to broken four-fold rotational symmetry.

- When the reflection symmetries are broken, an A_{2g} -like interaction operator $\Psi_{HO} \equiv V |\mathbb{1}\rangle \langle 0|$ mixes the $|0\rangle$ and $|\mathbb{1}\rangle$ states leading to two new local states:

$$|0_{HO}^L\rangle \approx \left(1 - \frac{V^2}{2\omega_0^2}\right) |0\rangle - \frac{V}{\omega_0} |\mathbb{1}\rangle \text{ and}$$

$$|0_{HO}^R\rangle \approx \left(1 - \frac{V^2}{2\omega_0^2}\right) |0\rangle + \frac{V}{\omega_0} |\mathbb{1}\rangle, \text{ with } V \text{ being the interaction strength.}$$

- When the reflection symmetries are broken, an A_{2g} -like interaction operator $\Psi_{\text{HO}} \equiv V |\mathbb{1}\rangle \langle 0|$ mixes the $|0\rangle$ and $|\mathbb{1}\rangle$ states leading to two new local states:

$$|0_{\text{HO}}^{\text{L}}\rangle \approx \left(1 - \frac{V^2}{2\omega_0^2}\right) |0\rangle - \frac{V}{\omega_0} |\mathbb{1}\rangle \text{ and}$$

$$|0_{\text{HO}}^{\text{R}}\rangle \approx \left(1 - \frac{V^2}{2\omega_0^2}\right) |0\rangle + \frac{V}{\omega_0} |\mathbb{1}\rangle, \text{ with } V \text{ being the interaction strength.}$$

- The choice of either the left-handed or the right-handed state on a given uranium site, $|0_{\text{HO}}^{\text{L}}\rangle$ or $|0_{\text{HO}}^{\text{R}}\rangle$, defines the local chirality in the HO phase

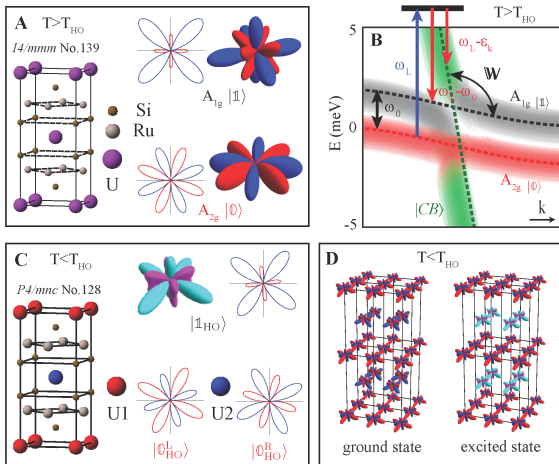


Figure : (D) Show schematics of chirality density wave, where the chiral states are staggered in the lattice (left). The right figure shows one of the possible excited state of the chirality density wave, where the chiral state $|0_{HO}^R\rangle$ at lattice site U2 is excited to $|1_{HO}\rangle$.

- A local order parameter of primary A_{2g} symmetry, breaking vertical/diagonal reflections, with subdominant B_{1g} component, breaking four-fold rotational symmetry, can be expressed in terms of the composite hexadecapole local order parameter of the form:

$$\pm V[(J_x - J_y)(J_x + J_y)(J_x J_y + J_y J_x) + (J_x J_y + J_y J_x)(J_x + J_y)(J_x - J_y)]$$

- A local order parameter of primary A_{2g} symmetry, breaking vertical/diagonal reflections, with subdominant B_{1g} component, breaking four-fold rotational symmetry, can be expressed in terms of the composite hexadecapole local order parameter of the form:

$$\pm V[(J_x - J_y)(J_x + J_y)(J_x J_y + J_y J_x) + (J_x J_y + J_y J_x)(J_x + J_y)(J_x - J_y)]$$

- where J_x , J_y are in-plane angular momentum operators

- A local order parameter of primary A_{2g} symmetry, breaking vertical/diagonal reflections, with subdominant B_{1g} component, breaking four-fold rotational symmetry, can be expressed in terms of the composite hexadecapole local order parameter of the form:

$$\pm V[(J_x - J_y)(J_x + J_y)(J_x J_y + J_y J_x) + (J_x J_y + J_y J_x)(J_x + J_y)(J_x - J_y)]$$

- where J_x , J_y are in-plane angular momentum operators
- A spatial order alternating the sign of this hexadecapole for neighboring basal planes is the chirality density wave that consistently explains the HO phenomena as it is observed by Raman and neutron scattering.

- The chirality density wave has no modulation of charge or spin and does not couple to tetragonal lattice, HENCE it is hidden to many probes

- The chirality density wave has no modulation of charge or spin and does not couple to tetragonal lattice, HENCE it is hidden to many probes
- The question of finding the hidden order WAS a hard one !

- The chirality density wave has no modulation of charge or spin and does not couple to tetragonal lattice, HENCE it is hidden to many probes
- The question of finding the hidden order WAS a hard one !
- Thank you for your attention !!